第 32 卷第 6 期 无 机 化 学 学 报 Vol.32 No.6
2016 年 6 月 CHINESE JOURNAL OF INORGANIC CHEMISTRY 1101-1110

咪唑–菲咯啉–苯氧乙酸锌、铅配合物的合成，结构及与 DNA 的相互作用

沈 伟[1] 胡未极[1] 吴小勇[1] 赵国良*,[1,2]
([1]浙江师范大学化学与生命科学学院，金华 321004)
([2]浙江师范大学行知学院，金华 321004)

摘要：以 2-4-(1*H*-咪唑-2-[4,5-*f*][1,10]菲咯啉基)苯氧乙酸(HPIMPHC)和 2-2-(1*H*-咪唑-2-[4,5-*f*][1,10]菲咯啉基)苯氧乙酸(HOIMPHC)为配体，水热合成了 2 种新型配合物[Zn(PIMPHC)$_2$]$_n$ (**1**)和{[Pb(OIMPHC)$_2$]·4H$_2$O}$_n$ (**2**)。配合物 **1** 属正交晶系，空间群为 *Pbcn*；Zn(Ⅱ)的配位数为 6，配位构型为变形的八面体，形成 2D 网状结构。配合物 **2** 属单斜晶系，空间群为 *P*2$_1$/*n*；Pb(Ⅱ)的配位数为 7，配位构型为变形的五角双锥，形成 2D 网状结构。荧光光谱的结果表明，配合物与 DNA 的相互作用强于配体。

关键词：2-4-(1*H*-咪唑-2-[4,5-*f*][1,10]菲咯啉基)苯氧乙酸；2-2-(1*H*-咪唑-2-[4,5-*f*][1,10]菲咯啉基)苯氧乙酸；Zn(Ⅱ)；Pb(Ⅱ)；DNA 作用
中图分类号：O614.24$^+$1；O614.43$^+$3 **文献标识码**：A **文章编号**：1001-4861(2016)06-1101-10
DOI：10.11862/CJIC.2016.132

Syntheses, Structures and DNA Interaction of Zn(Ⅱ) and Pb(Ⅱ) Complexes Based on Imidazo-phenanthrolin-phenoxy Acetic Acid

SHEN Wei[1] HU Wei-Ji[1] WU Xiao-Yong[1] ZHAO Guo-Liang*,[1,2]
([1]*College of Chemistry and Life Science, Zhejiang Normal University, Jinhua, Zhejiang* 321004, *China*)
([2]*Xingzhi College, Zhejiang Normal University, Jinhua, Zhejiang* 321004, *China*)

Abstract: Two novel complexes [Zn(PIMPHC)$_2$]$_n$ (**1**), {[Pb(OIMPHC)$_2$]·4H$_2$O}$_n$ (**2**) were synthesized under hydrothermal reactions by using 2-(4-(1*H*-imidazo-2-[4,5-*f*][1,10]phenanthrolinyl)phenoxy) acetic acid (HPIMPHC) and 2-(2-(1*H*-imidazo-2-[4,5-*f*][1,10]phenanthrolinyl)phenoxy) acetic acid (HOIMPHC). Complex **1** crystallizes in orthorhombic system with space group *Pbcn*. Zn(Ⅱ) is six-coordinated by two PIMPHC$^-$ anions, forming a distorted octahedral coordination geometry. Complex **2** crystallizes in monoclinic system with space group *P*2$_1$/*n*, Pb(Ⅱ) is seven-coordinated, forming a distorted pentagonal bipyramid coordination geometry. The fluorescence spectra indicate that the interaction of the complexes with DNA are stronger than ligands. CCDC: 1476033, **1**; 1476034, **2**.

Keywords: 2-(4-(1*H*-imidazo-2-[4,5-*f*][1,10]phenanthrolinyl)phenoxy) acetic acid; 2-(2-(1*H*-imidazo-2-[4,5-*f*][1,10]phenanthrolinyl) phenoxy) acetic acid; Zn(Ⅱ); Pb(Ⅱ); DNA-binding

Rational designs and syntheses of coordination polymers have attracted great interests in recent decades, owing to their rich structural aesthetics [1-5] and functionalities[6-9]. According to some factors of formation, molecular structures and properties of coordination polymers can be speculated, such as

收稿日期：2016-01-17。收修改稿日期：2016-04-23。
浙江省自然科学基金(No.LY12B01003)资助项目。
*通信联系人。E-mail：sky53@zjnu.cn

metal ions (nodes), ligands (linkers), metal-ligand ratio, supramolecular interaction, reaction conditions. Therefore, it is possible to develop a targeted architecture through the choice of organic ligands and metal ions.

So far, extensive work has been carried out by using heterocyclic carboxylate ligands[10-17], because these ligands containing both N- and O- donors are good choices to build multi-configurations. Carboxylate groups often play important roles in many organic ligands, which have different coordinating modes, such as monodentate terminal, bidentate bridging, bidentate chelating modes. The coordination modes make the expected structures much more robust. What is more, the flexibility of carboxylate groups offers the possibilities to form different topologies. Deprotonated carboxylate groups can form hydrogen bonds to participate in supermolecular self-assembly with coordination bonds as acceptors. Heterocyclic rings are expected to show robust coordination modes in the construction, and the π-π stacking interactions between heterocyclic rings make the whole framework further stable.

As is mentioned above, the advantages of heterocyclic carboxylate ligands offer a self-assembly solution that can be expected and controlled in certain extent. In this paper, two novel ligands (2-(4-(1*H*-imidazo-2-[4,5-*f*][1,10]phenanthrolinyl)phenoxy) acetic acid (HPIMPHC) and 2-(2-(1*H*-imidazo-2-[4,5-*f*][1,10]phenanthrolinyl)phenoxy) acetic acid (HOIMPHC)) were designed and synthesized, thereby two novel complexes ($[Zn(PIMPHC)_2]_n$ (**1**), $\{[Pb(OIMPHC)_2]\cdot 4H_2O\}_n$ (**2**)) were synthesized by hydrothermal reaction method. The interaction between complexes, ligands and ct-DNA were studied by EtBr fluorescence probe.

1 Experimental

1.1 Chemical and materials

All of the reagents were of analytical grade and used without further purification. Calf thymus DNA (ct-DNA) was prepared with 0.1 mol·L^{-1} NaCl. The concentration of ct-DNA was 200 μg·mL^{-1} (c_{DNA} = 3.72×10^{-4} mol·L^{-1}). The ct-DNA solutions were stored at 4 ℃ and gave a ratio of UV-Vis absorbance at 260 and 280 nm, A_{260}/A_{280}=1.8, indicating that DNA was sufficiently free of protein. The buffer solution, 0.01 mol·L^{-1} Tris-HCl (tris(hydroxymethyl) aminomethane hydrochloride (pH=7.4)), was prepared with double-distilled water.

Elemental analysis was performed on CHN elemental analyzer, Elementar Vario EL Ⅲ. FTIR spectra was recorded on a Nicolet NEXUS 670 FTIR spectrophotometer, using KBr discs in the range of 4 000~400 cm^{-1}. Crystallographic data of the complexes were collected on a Bruker Smart Apex Ⅱ CCD diffractometer. A Mettler Toledo thermal analyzer TGA/SDTA 851^e was used to carry out the thermoanalytical analysis with a heating rate of 10 ℃·min^{-1} from 30 to 800 ℃ in air atmosphere. Fluorescence spectra were measured at room temperature with an Edinburgh FL-FS920 TCSPC system. ^{1}H NMR spectra of ligands were acquired with Bruker AV400 NMR instrument in DMSO-d_6 solution with TMS as internal standard.

1.2 Synthesis of ligands

2-(4-(1*H*-imidazo-2-[4, 5-*f*][1, 10]phenanthrolinyl) phenoxy) acetic acid (HPIMPHC) and 2-(2-(1*H*-imidazo-2-[4,5-*f*][1,10]phenanthrolinyl)phenoxy) acetic acid (HOIMPHC) were synthesized according to literature(Fig.1)[18-20].

1.2.1 2-(4-formylphenoxy) acetic acid[18]

Chloracetic acid (2.5 mL, 50%) was added to 4-hydroxybenzaldehyde (1 g) and NaOH solution (3.5 mL, 33%), and gently heated on water bath (80 ℃) for 1 h. Then the mixture was immediately acidified with concentrated HCl, extracted with ether and 5% Na_2CO_3 solution. Na_2CO_3 extract was acidified with concentrated HCl. White powder was isolated and separated by filtration. The product thus obtained was recrystallized from ethanol. Yield: 86%.

1.2.2 1,10-phenanthroline-5,6-dione[19]

1,10-phenanthroline (1.20 g, 6 mmol) was added to concentrated H_2SO_4 (20 mL) and concentrated HNO_3 (10 mL) at 0 ℃. The mixture was refluxing at 80 ℃ for 2 h, then cooled to room temperature. The contents were diluted with deionized water (400 mL),

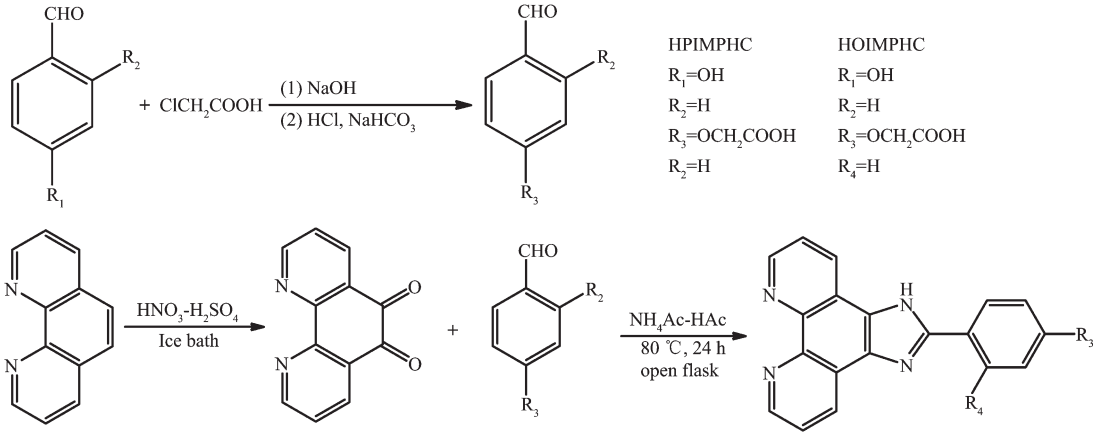

Fig.1　Synthesis of HPIMPHC and HOIMPHC

and neutralized with $NaHCO_3$, then extracted with methylene chloride, and dried over anhydrous Na_2SO_4. Yellow-brown powder was obtained. Yellow-brown crystals were recrystallized from methanol. Yield: 90%.

1.2.3　2-(4-(1*H*-imidazo[4,5-*f*][1,10]phenanthrolin-2-yl)phenoxy) acetic acid (HPIMPHC)[20]

1,10-phenanthroline-5,6-dione (5 mmol, 1.05 g) and 2-(4-formylphenoxy) acetic acid (5 mmol, 0.90 g) were added in the NH_4Ac-HAc buffer solution (10%, 20 mL). The mixture was heated in the open flask at 80 ℃. Deionized water was required to control the volume of solution. Yield: 80%. Anal. Calcd. for $C_{21}H_{13}N_4O_3$ (%): C, 68.29; H, 3.54; N, 15.17; Found (%): C, 68.25; H, 3.58; N, 15.23. IR (KBr, cm^{-1}): 3 418 (br), 2 358(w), 1 611(s), 1 579(m), 1 559(m), 1 538 (m), 1484(m), 1 458(m), 1 422(m), 1 362(w), 1 338(w), 1 315(w), 1 295(w), 1 254(m), 1 190(m), 1 127(w), 1 059(m), 958(w), 846(w), 822(w), 742(w), 721(m), 694 (w). ^{1}H NMR (400MHz, DMSO-d_6): δ 8.90~9.03 (4H) for phenanthroline-H, 7.83~7.84(2H) for phenanthroline-H, 7.17~7.19 (2H) for benzene-H, 8.21~8.23 (2H) for benzene-H, 4.83(2H, s, -CH_2-), 13.66(H, -OH).

1.2.3　2-(2-(1*H*-imidazo[4,5-*f*][1,10]phenanthrolin-2-yl)phenoxy) acetic acid (HOIMPHC)

The synthetic process of HOIMPHC is the same as HPIMPHC. 2-hydroxybenzaldehyde was used instead of 4-hydroxybenzaldehyde. Yellow-brown powder was recrystallized from methanol. Yield: 70.1%, Anal. Calcd. for $C_{21}H_{13}N_4O_3$(%): C, 68.29; H, 3.54; N, 15.17; Found(%): C, 68.22; H, 3.53; N, 15.32. IR(KBr, cm^{-1}): 3 440(br), 2 362(w), 1 680(s), 1 584(m), 1 562(m), 1 544 (m), 1488(m), 1 462(m), 1 433(m), 1 375(w), 1 345(w), 1 323(w), 1 294(w), 1 252(m), 1 195(m), 1132(w), 1 065 (m), 959(w), 841(w), 805(w), 752(w), 735(m), 704(w). ^{1}H NMR (400 MHz, DMSO-d_6): δ 8.42~8.94 (4H) for phenanthroline-H, 7.73~7.79 (2H) for phenanthroline-H, 7.15, 7.24, 7.51, 7.76(4H) for benzene-H, 4.76(2H, s, -CH_2-), 14.45 (H, -OH).

1.3　Synthesis of complexes

$[Zn(PIMPHC)_2]_n$ (**1**): A mixture of HPIMPHC (0.148 g, 0.4 mmol), NaOH (0.016 g, 0.4 mmol), $ZnSO_4 \cdot 7H_2O$ (0.058 g, 0.2 mmol), and H_2O/EtOH (20 mL, 1∶1, *V*/*V*) was sealed in a 25 mL Teflon-lined stainless steel vessel and heated at 160 ℃ for 3 d. Then the mixture was cooled to room temperature at a rate of 10 ℃·h^{-1}, with colorless crystals appearing at the bottom of the Teflon vessel. After washed with distilled water and dried in air, the crystals suitable for single-crystal analysis and physical measurements were obtained. Yield: 45% (based on HPIMPHC). Anal. Calcd. for $C_{42}H_{26}N_8O_6Zn$(%): C, 62.68; H, 3.23; N, 13.93; Found (%): C, 62.54; H, 3.19; N, 13.87; IR (KBr, cm^{-1}): 3 072(w), 2 354(w), 1 608(s), 1 527(m), 1 479(s), 1 454(m), 1 362(m), 1 075(m), 837(m), 812 (m), 733(m), 694(m), 635(m).

$\{[Pb(OIMPHC)_2]\cdot 4H_2O\}_n$ (**2**): The preparation of **2** was similar to **1** using HOIMPHC and $Pb(NO_3)_2$ instead of HPIMPHC and $ZnSO_4 \cdot 7H_2O$. Yield: 38% (based on HOIMPHC). Anal. Calcd. for $C_{42}H_{34}N_8O_{10}Pb$(%): C, 49.51; H, 3.34; N, 11.00; Found (%): C, 49.40; H, 3.29; N, 10.96; IR(KBr, cm^{-1}): 3 424(w), 2 361(w), 1 607

(s), 1 514(s), 1 481(s), 1 446(m), 1 388(m), 1 358(m), 1 259(m), 1 224(m), 1 067(m), 836(m), 817(m), 740 (m), 701(m), 638(m).

1.4 Single X-ray crystallographic study

The single crystal of the complexes with approximate dimensions were mounted on a Bruker Smart Apex CCD diffractometer. A graphite monochromated Mo $K\alpha$ radiation (λ=0.071 073 nm) was used to collect the diffraction data at 296 K. The structures were solved by SHELXS-97 program package[21-22] and refined with the full-matrix least-squares technique based on F^2 using the SHELXTL-97 program package[23]. All non-H atoms were anisotropically refined. Remaining hydrogen atoms were added in calculated positons and refined as riding atoms with a common fixed isotropic thermal parameter. Hydrogen atoms on water molecules were located in a difference Fourier map and included in the subsequent refinement using restrains (d(O-H)= 0.085 nm) with U_{iso}(H)=1.5 U_{eq}(O). Detail information about the crystal data is summarized in Table 1. Selected interatomic distances and bond angles are given in Table 2 and Table 3.

CCDC: 1476033, **1**; 1476034, **2**.

Table 1 Crystallographic data for complex 1 and complex 2

Complex	1	2
Empirical formula	$C_{42}H_{36}N_8O_6Zn$	$C_{42}H_{34}N_8O_{10}Pb$
Formula weight	804.08	1 017.96
Crystal system	Orthorhombic	Monoclinic
Space group	*Pbcn*	$P2_1/n$
a / nm	1.822 57(1)	0.738 25(2)
b / nm	1.031 12(6)	3.165 51(1)
c / nm	1.946 89(1)	1.639 73(8)
β / (°)		92.427(2)
V / nm^3	3 658.8(4)	3 828.5(2)
Z	4	4
D_c / (g·cm^{-3})	1.460	1.766
Absorption coefficient / mm^{-1}	0.734	4.481
Crystal size / mm	0.201×0.149×0.096	0.192×0.125×0.083
F(000)	1 648	2 016
θ_{min}, θ_{max} / (°)	2.372, 22.210	2.484, 22.716
Reflections collected	16 392	34 763
Unique reflections	3 709	8 823
Observed reflections	2 190	6 048
R_{int}	0.071 4	0.048 4
R indices [I>2σ(I)]	R_1=0.046 3, wR_2=0.103 0	R_1=0.039 9, wR_2=0.086 2
R indices (all data)	R_1=0.093 5, wR_2=0.121 5	R_1=0.072 7, wR_2=0.106 1
Goodness-of-fit (on F^2)	1.001	1.054
$(\Delta\rho)_{max}$, $(\Delta\rho)_{min}$ / (e·nm^{-3})	336, −338	1 068, −1 461

Table 2 Selected bond lengths (nm) and angle (°) for 1

Zn(1)-O(2)^{i}	0.203 4(2)	Zn(1)-N(2)^{iii}	0.220 1(2)	Zn(1)-N(1)	0.221 2(3)
Zn(1)-O(2)^{ii}	0.203 4(2)	Zn(1)-N(2)	0.220 1(2)	Zn(1)-N(1)^{iii}	0.221 2(3)
O(2)^{i}-Zn(1)-O(2)^{ii}	89.88(13)	O(2)^{i}-Zn(1)-N(1)^{iii}	92.02(9)	N(2)^{iii}-Zn(1)-N(2)	155.50(14)
O(2)^{ii}-Zn(1)-N(2)^{iii}	91.02(9)	N(2)^{iii}-Zn(1)-N(1)^{iii}	75.42(9)	O(2)^{ii}-Zn(1)-N(1)	92.02(9)
O(2)^{ii}-Zn(1)-N(2)	106.42(9)	N(1)-Zn(1)-N(1)^{iii}	89.35(14)	N(2)-Zn(1)-N(1)	75.42(9)

Continued Table 2

O(2)^{i}-Zn(1)-N(1)	166.29(8)	O(2)^{i}-Zn(1)-N(2)^{iii}	106.42(9)	O(2)^{ii}-Zn(1)-N(1)^{iii}	166.29(8)
N(2)^{iii}-Zn(1)-N(1)	87.13(9)	O(2)^{i}-Zn(1)-N(2)	91.02(9)	N(2)-Zn(1)-N(1)^{iii}	87.13(9)

Symmetry codes: ^{i} $-x+3/2, -y+3/2, z+1/2$; ^{ii} $x+1/2, -y+3/2, -z+1$; ^{iii} $-x+2, y, -z+3/2$.

Table 3　Selected bond lengths (nm) and angle (°) for 2

Pb(1)-N(1)	0.253 5(4)	Pb(1)-N(4)	0.259 2(4)	Pb(1)-O(5)^{ii}	0.281 4(4)
Pb(1)-N(3)	0.258 1(4)	Pb(1)-O(2)^{i}	0.281 6(4)		
Pb(1)-N(2)	0.258 8(4)	Pb(1)-O(4)^{ii}	0.299 8(3)		
N(1)-Pb(1)-N(3)	88.52(14)	N(2)-Pb(1)-N(4)	134.32(14)	O(2)^{i}-Pb(1)-N(4)	85.85(12)
N(1)-Pb(1)-N(2)	64.46(13)	O(4)^{ii}-Pb(1)-O(5)^{ii}	44.94(13)	O(4)^{ii}-Pb(1)-N(4)	74.93(12)
N(3)-Pb(1)-N(2)	83.86(13)	O(2)i-Pb(1)-O(4)^{ii}	117.63(12)	O(4)^{ii}-Pb(1)-N(1)	75.54(12)
N(1)-Pb(1)-N(4)	82.46(13)	O(2)^{i}-Pb(1)-O(5)^{ii}	130.65(12)	O(5)^{ii}-Pb(1)-N(2)	80.88(12)
N(3)-Pb(1)-N(4)	63.75(13)	O(2)^{i}-Pb(1)-N(3)	71.02(12)	O(5)^{ii}-Pb(1)-N(1)	70.01(12)

Symmetry codes: ^{i} $x+0.5, -y+0.5, z+0.5$; ^{ii} $x+0.5, -y+1/2, z-0.5$.

2　Results and discussion

2.1　Crystal structure of $[Zn(PIMPHC)_2]_n$ (1)

Single-crystal analysis shows that **1** crystallizes in orthorhombic system with space group *Pbcn*. The asymmetric unit cell contains one Zn(Ⅱ) ion and two PIMPHC$^-$ anions. The Zn(Ⅱ) exhibits distorted six-coordinated geometry by considering short-range atomic interactions. Each Zn(Ⅱ) is bound to four nitrogen atoms (N1, N2, N1^{iii}, N2^{iii}, Zn-N 0.220 1(2)~0.221 2(3) nm) and two oxygen atoms(O2^{i}, O2^{ii}, Zn-O 0.203 4(2) nm). PIMPHC$^-$ adopts a μ^2-κO:κ_2N coordination fashion to connect two Zn(Ⅱ) ions. The selected distances and bond angles for complex **1** fall in the normal regions which are comparable to the values reported in literatures[24-26].

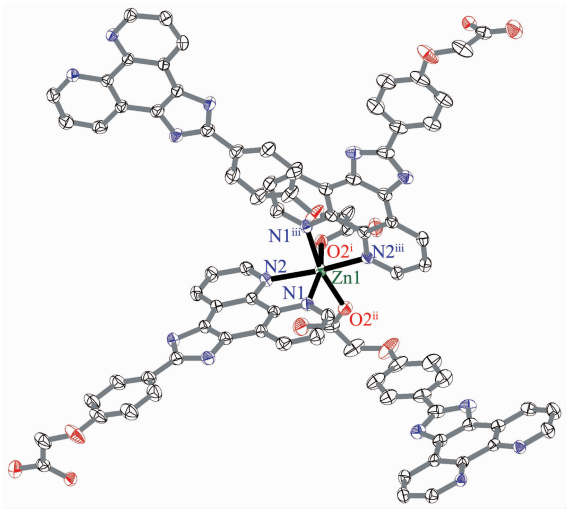

Ellipsoidal probability level: 30%; Symmetry codes: ^{i} $-x+3/2, -y+3/2, z+1/2$; ^{ii} $x+1/2, -y+3/2, -z+1$; ^{iii} $-x+2, y, -z+3/2$

Fig.2　Coordinated environment of complex **1**

In the μ^2-κO :κ_2N coordination fashion, the phenanthroline unit chelates to one Zn(Ⅱ) and the deprotonated carboxylate unit is bound to another. The coordination mode of the μ^2-PIMPHC$^-$ forms metallacyclic rings, which can be described as a 2D (2,4)-connected binodal network with the Schläfli symbol of $(8^4\cdot12^2)^2\cdot(8)^2$. Every plane is parallel to each other. Through $\pi\cdots\pi$ stacking interaction of ligands and hydrogen bonds, 2D polymers form 3D structures.

2.2　Crystal structure of $\{[Pb(OIMPHC)_2]\cdot4H_2O\}_n$ (2)

Single-crystal analysis shows that **2** crystallizes in monoclinic crystallographic system with space group $P2_1/n$. The asymmetric unit cell contains one Pb(Ⅱ) ion, two crystallographically independent OIMPHC$^-$ anions and four water molecules. The Pb(Ⅱ) exhibits highly distorted seven-coordinated geometry by considering short-range atomic interactions. Each Pb(Ⅱ) is bound to four nitrogen atoms (N1, N2, N3, N4, Pb-N 0.253 5(4)~0.259 2(4) nm) and three oxygen atoms (O2, O4, O5, Pb-O 0.281 4(4)~0.299 8(3) nm) of ligands. OIMPHC$^-$ adopts μ^2-κO:κ^2N and μ^2-κ^2O:κ^2N coordination fashions to connect two Pb(Ⅱ) ions. The

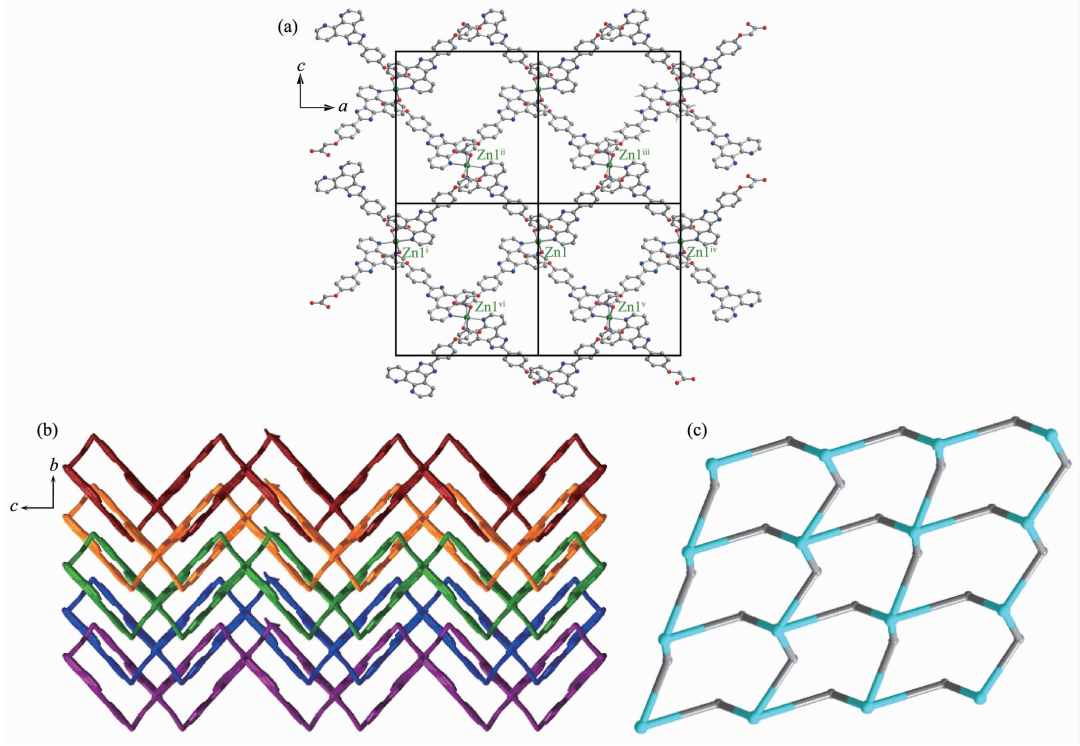

Symmetry codes: [i] −1+*x*, *y*, *z*; [ii] 1.5−*x*, 1.5−*y*, 0.5+*z*; [iii] 2.5−*x*, 1.5−*y*, 0.5+*z*; [iv] 1+*x*, *y*, *z*; [v] 2.5−*x*, 1.5−*y*, −0.5+*z*; [vi] 1.5−*x*, 1.5−*y*, −0.5+*z*

Fig.3 (a) Single-layer 2D structure of complex **1**; (b) 3D packing diagram of complex **1**; (c) 2D topological structure of complex **1**

selected distances and bond angles for complex **2** fall in the normal regions which are comparable to the values reported in literatures[27-32]. In μ^2-κO:κ^2N coordination fashion, the phenanthroline unit chelates to one Pb(Ⅱ) ion and the deprotonated carboxylate unit is bound to another. In μ^2-κ^2O:κ^2N coordination fashion, the phenanthroline unit chelates to one Pb(Ⅱ), and the deprotonated carboxylate unit chelates to another. These coordination modes forms metallacyclic rings, which can be described as a 2D (2,2,3) network with the Schläfli symbol of $(8^3)^2\cdot(8)$. Every plane is parallel to each other.

In the 2D polymers, the coordinating competition between phenanthroline unit and carboxylate unit need to be considered. To simplify the demonstration, the ligand coordinated by one oxygen atom and two nitrogen atoms(O2, N1, N2) is labelled as A, the other as B. The different coordinating modes result in the considerable dihedral anglar difference between the benzene ring and the phenanthroline ring. The dihedral angle of A and B are 0.980° and 5.299°, respectively, which are attributed to different coordinating modes of ligands. One interpretation may be attributed to π-π stacking interactions between conjugate rings of ligands. The distance between adjacent imidazo-phenanthroline rings is 0.337 5 nm. According to Table 3, Bond distances of Pb-O are much longer than usual (Pb1-O2[i] 0.281 6(4) nm, Pb1-O4[ii] 0.299 8(3) nm, Pb1-O5[ii] 0.281 4(4) nm). The long Pb-O bonds can be ascribed to different coordinating modes as five-member chelating mode is much stronger than monodentate mode and four-member chelating mode. While the four-member chelating mode still has some effects on the structure, some toision angles (Pb1-N1-C15-C16 23.9(5)°, Pb1-N2-

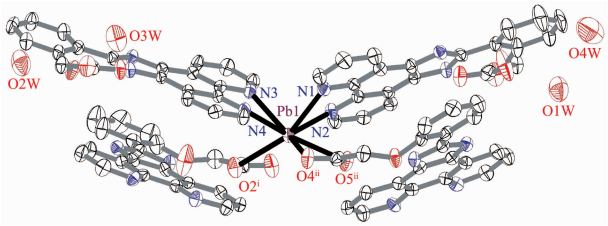

Ellipsoidal probability level: 30%; Symmetry codes: [i] 0.5+*x*, 0.5−*y*, 0.5+*z*; [ii] 0.5+*x*, 0.5−*y*, −0.5+*z*

Fig.4 Coordinated environment of complex **2**

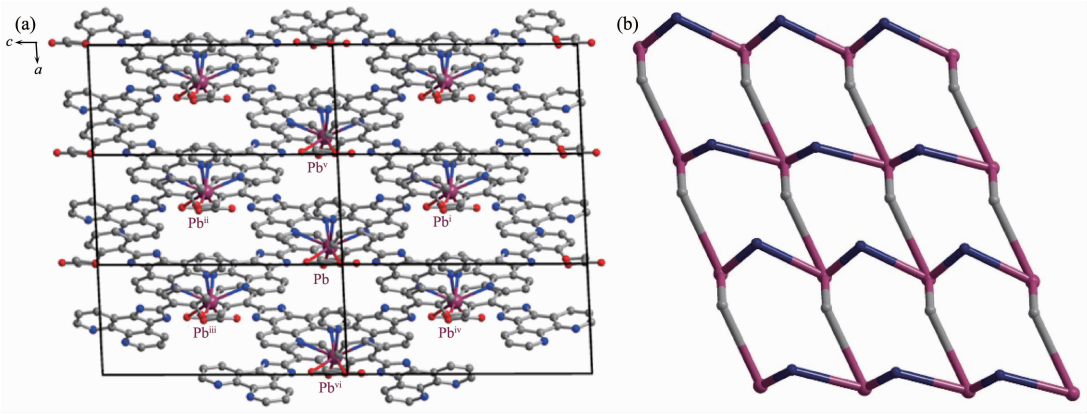

Symmetry codes: ^{i} −0.5+x, 0.5−y, −0.5+z; ^{ii} −0.5+x, 0.5−y, 0.5+z; ^{iii} 0.5+x, 0.5−y, 0.5+z; ^{iv} 0.5+x, 0.5−y, −0.5+z; ^{v} −1+x, y, z; ^{vi} 1+x, y, z

Fig.5　(a) 2D structure of complex **2**; (b) Topological structure of complex **2**

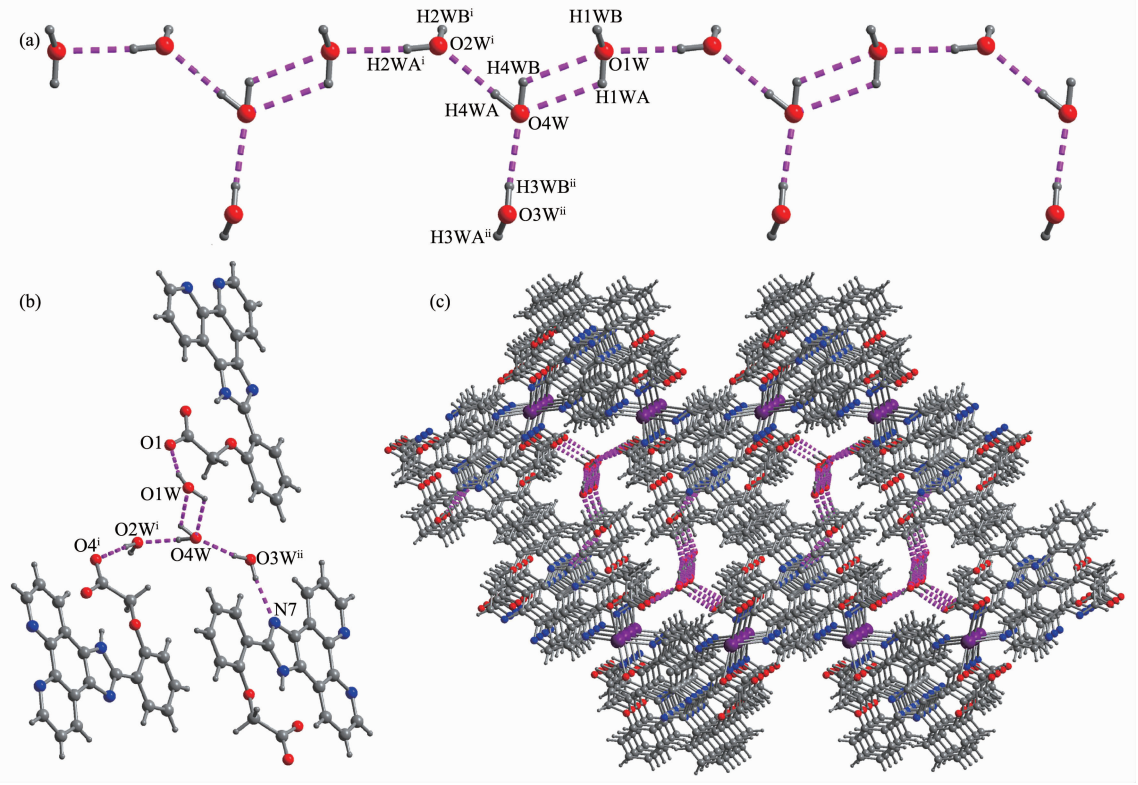

Symmetry codes: ^{i} −0.5+x, 0.5−y, −1.5+z; ^{ii} 0.5−x, 0.5+y, −0.5−z

Fig.6　(a) 1D water chain of complex **2**; (b) Ligands linked via hydrogen bonds; (c) Hydrogen-bonded packing diagram of complex **2**

C16-C15 −23.1(5)°, Pb1-N3-C35-C36 22.9(5)°, Pb1-N4-C36-C35 −20.9(5)°) can be recognized.

A self-assemble chain of water molecules (O2W^{i}–H2WA^{i}⋯O1W^{iv}, O1W–H1WA⋯O4W, O4W–H4WA⋯O2W^{i}, O4W–H4WB⋯O1W, O3W^{ii}–H3WB^{ii}⋯O4W) are observed in Table 4. Water chains are fixed by hydrogen bonds (O1W–H1WB⋯O1^{iii}, O2W^{i}–H2WB^{i}⋯O4^{i}, O3W^{ii}–H3WA^{ii}⋯N7^{ii}) and interconnect adjacency 2D networks to form 3D constructures. A side view of the same part of the structure along the direction is shown in Fig.6(c), where water chains parallel to this direction and crossing into the space of 2D networks are clearly seen.

2.3　IR analysis

The stretching vibration of C=O (1 611 cm^{-1}) for HPIMPHC is much smaller than usual[33], which may be owing to intermolecular hydrogen bonds among carboxylate groups. In complex **1**, This characteristic

Table 4 Hydrogen bond distances (nm) and angles (°) in complex 2

D–H···A	*d*(D-H) / nm	*d*(H···A) / nm	*d*(D···A) / nm	∠DHA / (°)
O(1W)–H(1WA)···O(4W)	0.087	0.235	0.281 2(7)	113.2
O(1W)–H(1WB)···O(1)^{iii}	0.085	0.198	0.279 6(6)	160.0
O(2W)^{i}–H(2WA)^{i}···O(1W)^{iv}	0.085	0.208	0.292 2(7)	172.4
O(2W)^{i}–H(2WB)^{i}···O(4)^{i}	0.085	0.199	0.283 3(5)	171.8
O(3W)^{ii}–H(3WA)^{ii}···N(7)^{ii}	0.085	0.213	0.297 2(6)	170.2
O(3W)^{ii}–H(3WB)^{ii}···O(4W)	0.085	0.232	0.294 9(7)	131.0
O(4W)–H(4WA)···O(2W)^{i}	0.085	0.249	0.285 5(7)	106.8
O(4W)–H(4WB)···O(1W)	0.085	0.232	0.281 2(7)	116.9

Symmetry codes: ^{i} $x-0.5, -y+0.5, z-1.5$; ^{ii} $-x+0.5, y+0.5, -z-0.5$; ^{iii} $x, y, z+1$; ^{iv} $x-1, y-1, z-1$.

stretching vibration of C=O and O-H are absent and the asymmetric and symmetric stretchings of COO^- appear at 1 608 cm^{-1} ($\nu(OCO)_{asym}$) and 1 362 cm^{-1} ($\nu(OCO)_{sym}$) respectively, showing the presence of mono-dentate carboxylate linkage. The C=N characteristic stretching vibration of HPIMPHC is 1 483 cm^{-1}, while it shifts to 1 479 cm^{-1} in complex **1**. It is concluded that the chelating mode of phenanthroline groups reduces the frequency of C=N stretching vibration.

So is the complex **2**, the characteristic stretching vibrations of O-H and C=O for HOIMPHC are absent and the asymmetric and symmetric stretchings of COO^- appear at 1 607 cm^{-1} ($\nu(OCO)_{asym}$), 1 388 cm^{-1} ($\nu(OCO)_{sym}$) and 1 358 cm^{-1} ($\nu(OCO)_{sym}$) respectively, which shows the presence of two different carboxylate linkage. The carboxylate groups act as both bidenate and monodenate coordination modes. The C=N characteristic stretching vibration of HOIMPHC is 1 483 cm^{-1}, while it shifts to 1 481 cm^{-1} in complex **2**, which is similar to complex **1**.

2.4 Thermal decomposition of complexes

The TG curves of the title complexes are shown in Fig.7. No weight loss of complex **1** was observed below 200 ℃, indicating that there is no small solvent molecules in complex **1**. The decomposition of complex **1** starts at 200 ℃ and ended at 440 ℃, and the observed weight loss (89.98%) accompanied with the decomposition of $PIMPHC^-$ (Calcd. 89.88%). The residual weight 10.02% might correspond to ZnO (Calcd. 10.12%). Complex **2** experiences two steps of weight loss. The first step is from 72 to 129 ℃ with a weight loss of 7.17%, which corresponds to the loss of four water molecules (Calcd. 7.07%). The second step in the range of 220~527 ℃ with a weight loss of 71.14% corresponds to the decomposition of $OIMPHC^-$ (Calcd. 71.00%). Finally, the remaining weight of 21.69%, seems likely to correspond to PbO (Calcd. 21.93%).

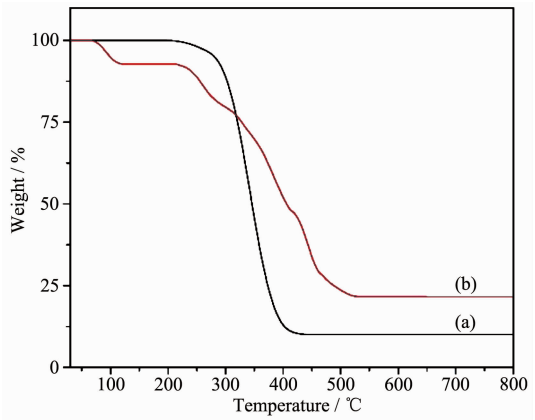

Fig.7 TG curves for complex **1** (a) and **2** (b)

2.5 EB-DNA binding study by fluorescence spectrum

The effects of the ligands and complexes on the fluorescence spectra of EB-DNA system are presented in Fig.8, the fluorescence intensities of EB bound to ct-DNA at 592 nm show remarkable decreasing trends with the increasing concentration of the complexes, indicating that some EB molecules are released into solution after the exchange with the compounds which resulted in the fluorescence quenching of EB. The quenching of EB bound to DNA by the compounds is in agreement with the linear Stern-Volmer equation: $I_0/I=1+K_{sq}r$[34], where I_0 and I represent the fluorescence intensities in the absence and presence of quencher, respectively. K_{sq} is the linear Stern-Volmer quenching

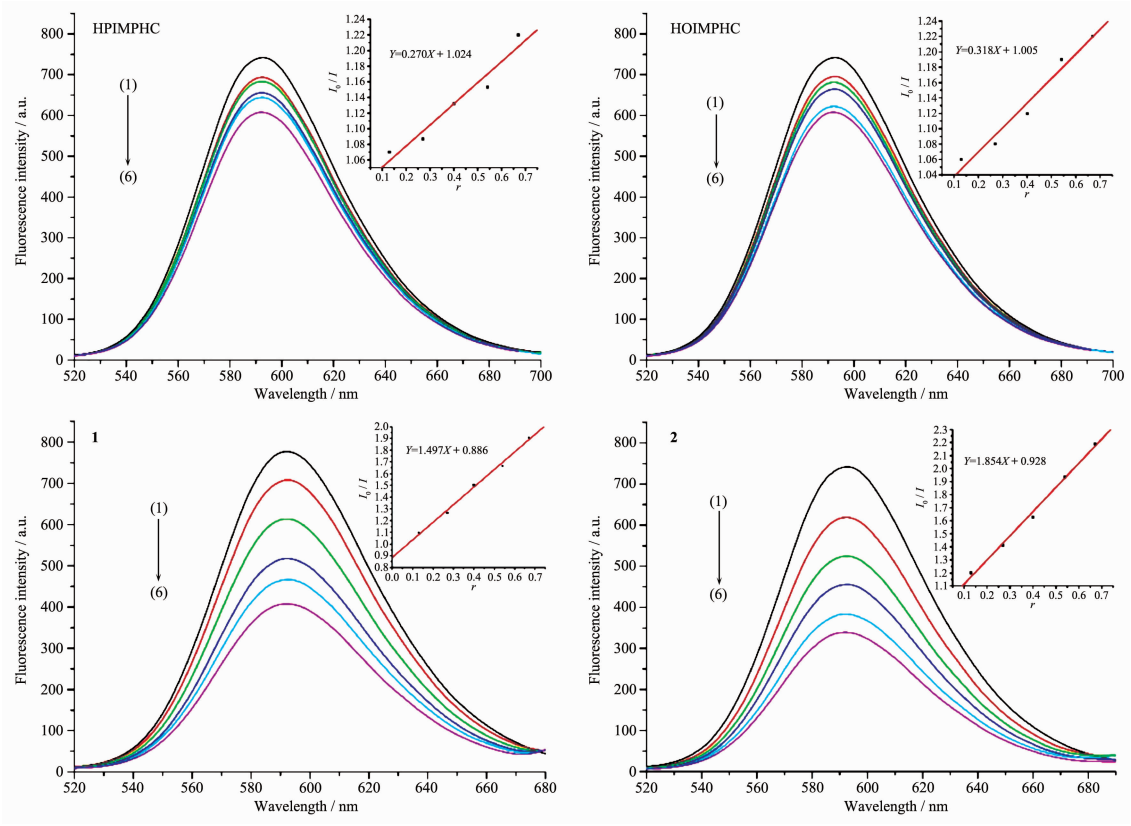

(1) r=0; (2) r=0.13; (3) r=0.27; (4) r=0.4; (5) r=0.54; (6) r=0.67; Inset: plot of I_0/I versus r

Fig.8　Emission spectra of EB-DNA system in the absence and presence of ligands and complexes

constant, r is the ratio of the concentration of quencher and DNA. In the quenching plots (insets in Fig.8) of I_0/I versus r, K_{sq} values are given by the slopes. The K_{sq} values for the compounds are 0.270, 1.497 for HPIMPC and complex **1**, 0.318, 1.854 for HOIMPC and complex **2**, respectively. The results indicate that interaction of the complexes with DNA are stronger than ligands, because the complexes have higher rigidity to bind the base pairs along DNA, thus increasing their binding abilities.

3　Conclusions

In summary, new ligands HPIMPHC and HOIMPHC were purposely synthesized based on 1, 10-phenanthroline. Both of ligands were successfully applied to constructing $[Zn(PIMPHC)_2]_n$ (**1**), $\{[Pb(OIMPHC)_2]\cdot 4H_2O\}_n$ (**2**). The complex **1** is a 2D framework with (2,4)-connected topology. The complex **2** is a 2D framework with (2,2,4)-connected topology. Because of the competition among monodentate mode, four-member chelating mode and five-member chelating mode, bond distances of Pb-O are much longer than usual. Complex **2** has stronger interaction with DNA, which can release more free EB molecules from EB-DNA.

References:

[1] Li H J, Zhao B, Ding R, et al. *Cryst. Growth Des.*, **2012**,**12**(8):4170-4179

[2] Lin J D, Cheng J W, Du S W. *Cryst. Growth Des.*, **2008**,**8**(9):3345-3353

[3] Venkataraman D, Gardner G B, Lee S, et al. *J. Am. Chem. Soc.*, **1995**,**117**(46):11600-11601

[4] Batten S R, Robson R. *Angew. Chem. Int. Ed.*, **1998**,**37**(11):1460-1494

[5] James S L. *Chem. Soc. Rev.*, **2003**,**32**(5):276-288

[6] Huang Z, White P S, Brookhart M. *Nature*, **2010**,**465**(7298):598-601

[7] Lü L L, Yang J, Zhang H M, et al. *Inorg. Chem.*, **2015**,**54**(4):1744-1755

[8] Wang J C, Liu Q K, Ma J P, et al. *Inorg. Chem.*, **2014**,**53**(20):10791-10793

[9] Gong Y N, Huang Y L, Jiang L, et al. *Inorg. Chem.*, **2014**,**53**(18):9457-9459

[10]Panella B, Hirscher M, Pütter H, et al. *Adv. Funct. Mater.*, **2006**,**16**(4):520-524

[11]Stock N, Biswas S. *Chem. Rev.*, **2011**,**112**(2):933-969

[12]Arstad B, Fjellvg H, Kongshaug K O, et al. *Adsorption*, **2008**, **14**(6):755-762

[13]Janiak C, Vieth J K. *New J. Chem.*, **2010**,**34**(11):2366-2388

[14]Henninger S K, Habib H A, Janiak C. *J. Am. Chem. Soc.*, **2009**,**131**(8):2776-2777

[15]Torrisi A, Bell R G, Mellot-Draznieks C. *Cryst. Growth Des.*, **2010**,**10**(7):2839-2841

[16]Li K, Olson D H, Lee J Y, et al. *Adv. Funct. Mater.*, **2008**, **18**(15):2205-2214

[17]Lee C Y, Farha O K, Hong B J, et al. *J. Am. Chem. Soc.*, **2011**,**133**(40):15858-15861

[18]Nikalje A P G, Deshpande D, Une H D. *Eur. J. Exp. Biol.*, **2012**,**2**:343-353

[19]Guo W, Engelman B J, Haywood T L, et al. *Talanta*, **2011**, **87**:276-283

[20]Lee Y S, Cho Y H, Lee S J, et al. *Tetrahedron*, **2015**,**71**(4): 532-538

[21]Scheldrick G M. *SADABS*, University of Göttingen, Göttingen, Germany, **1996**.

[22]Sheldrick G M. *SHELXS*-97, *Program for the Solution of Crystal Structure*, University of Göttingen, Göttingen, Germany, **1997**.

[23]Sheldrick G M. *SHELXTL*-97, *Program for the Refinement of Crystal Structure*, University of Göttingen, Göttingen, Germany, **1997**.

[24]Starikov A G, Minkin V I, Minyaev R M, et al. *J. Phys. Chem. A*, **2010**,**114**(29):7780-7785

[25]Ivakhnenko E P, Starikov A G, Minkin V I, et al. *Inorg. Chem.*, **2011**,**50**(15):7022-7032

[26]Tian Z, Lin J, Su Y, et al. *Cryst. Growth Des.*, **2007**,**7**(9): 1863-1867

[27]Alvarado R J, Rosenberg J M, Andreu A, et al. *Inorg. Chem.*, **2005**,**44**(22):7951-7959

[28]Kavallieratos K, Rosenberg J M, Bryan J C. *Inorg. Chem.*, **2005**,**44**(8):2573-2575

[29]Gabriel C, Vangelis A A, Raptopoulou C P. *Cryst. Growth Des.*, **2015**,**15**(11):5310-5326

[30]Peedikakkal A M P, Vittal J J. *Cryst. Growth Des.*, **2011**,**11** (10):4697-4703

[31]TANG Long(唐龙), WU Ya-Pan(吴亚盘), FU Feng(付峰), et al. *Chinese J. Inorg. Chem.*(无机化学学报), **2011**,**27**(11): 2287-2290

[32]LI Chun-Xiang(李春香), WANG Jian(王艰), LIU Chun-Bo (刘春波), et al. *Chinese J. Inorg. Chem.*(无机化学学报), **2009**,**25**(12):2211-2214

[33]Larkin P. *Infrared and Raman Spectroscopy*: *Principles and Spectral Interpretation*. Waltham: Elsevier, **2011**.

[34]Lakowicz J R, Weber G. *Biochemistry*, **1973**,**12**(21):4161-4170